An aberrant NOTCH2-BCR signaling axis in B cells from patients with chronic GVHD

Jonathan C. Poe,[1,*] Wei Jia,[1,*] Hsuan Su,[1] Sarah Anand,[1] Jeremy J. Rose,[2] Prasanthi V. Tata,[3] Amy N. Suthers,[1] Corbin D. Jones,[4] Pei Fen Kuan,[5] Benjamin G. Vincent,[3] Jonathan S. Serody,[3] Mitchell E. Horwitz,[1] Vincent T. Ho,[6] Steven Z. Pavletic,[2] Frances T. Hakim,[2] Kouros Owzar,[7] Dadong Zhang,[7] Bruce R. Blazar,[8,9] Christian W. Siebel,[10] Nelson J. Chao,[1] Ivan Maillard,[11,12] and Stefanie Sarantopoulos[1]

[1]Division of Hematologic Malignancies and Cellular Therapy, Department of Medicine, Duke Cancer Institute, Duke University Medical Center, Durham, NC; [2]Experimental Transplantation and Immunology Branch, National Cancer Institute, National Institutes of Health, Bethesda, MD; [3]Department of Medicine, Lineberger Comprehensive Cancer Center, University of North Carolina, Chapel Hill, NC; [4]Department of Biology, University of North Carolina, Chapel Hill, NC; [5]Department of Applied Mathematics and Statistics, Stony Brook University, Stony Brook, NY; [6]Division of Hematologic Malignancies, Department of Medical Oncology, Dana-Farber Cancer Institute, Boston, MA; [7]Department of Biostatistics and Bioinformatics, Duke Cancer Institute, Duke University Medical Center, Durham, NC; [8]Division of Blood and Marrow Transplantation, Department of Pediatrics and [9]Masonic Cancer Center, University of Minnesota, Minneapolis, MN; [10]Department of Discovery Oncology, Genentech, Inc, South San Francisco, CA; and [11]Life Sciences Institute and [12]Division of Hematology-Oncology, Department of Internal Medicine, University of Michigan, Ann Arbor, MI

Key Points

- NOTCH2 activation confers a marked increase in BCR responsiveness by cGVHD patient B cells that associates with increased BLNK.
- ATRA increases the IRF4-to-IRF8 ratio and blocks aberrant NOTCH2-BCR activation without affecting cGVHD patient B-cell viability/function.

B-cell receptor (BCR)-activated B cells contribute to pathogenesis in chronic graft-versus-host disease (cGVHD), a condition manifested by both B-cell autoreactivity and immune deficiency. We hypothesized that constitutive BCR activation precluded functional B-cell maturation in cGVHD. To address this, we examined BCR-NOTCH2 synergy because NOTCH has been shown to increase BCR responsiveness in normal mouse B cells. We conducted ex vivo activation and signaling assays of 30 primary samples from hematopoietic stem cell transplantation patients with and without cGVHD. Consistent with a molecular link between pathways, we found that BCR-NOTCH activation significantly increased the proximal BCR adapter protein BLNK. BCR-NOTCH activation also enabled persistent NOTCH2 surface expression, suggesting a positive feedback loop. Specific NOTCH2 blockade eliminated NOTCH-BCR activation and significantly altered NOTCH downstream targets and B-cell maturation/effector molecules. Examination of the molecular underpinnings of this "NOTCH2-BCR axis" in cGVHD revealed imbalanced expression of the transcription factors *IRF4* and *IRF8*, each critical to B-cell differentiation and fate. All-*trans* retinoic acid (ATRA) increased *IRF4* expression, restored the *IRF4*-to-*IRF8* ratio, abrogated BCR-NOTCH hyperactivation, and reduced NOTCH2 expression in cGVHD B cells without compromising viability. ATRA-treated cGVHD B cells had elevated *TLR9* and *PAX5*, but not *BLIMP1* (a gene-expression pattern associated with mature follicular B cells) and also attained increased cytosine guanine dinucleotide responsiveness. Together, we reveal a mechanistic link between NOTCH2 activation and robust BCR responses to otherwise suboptimal amounts of surrogate antigen. Our findings suggest that peripheral B cells in cGVHD patients can be pharmacologically directed from hyperactivation toward maturity. (*Blood*. 2017;130(19):2131-2145)

Introduction

The most devastating long-term side effect of allogeneic hematopoietic stem cell transplantation (HCT) is chronic graft-versus-host disease (cGVHD).[1,2] Incited by recipient alloantigens, cGVHD evolves into a recalcitrant autoreactive and immunocompromised state.[3,4] Aberrantly activated T and B cells are found in patients.[5-9] Specific roles for these cells in cGVHD pathogenesis have been substantiated in mouse models, leading to clinical trials.[2,10,11] Despite these advances, inadequate understanding of immune mechanisms in human cGVHD hinders our ability to prevent and treat cGVHD without further compromising immunity.

Both cGVHD patients and mice have increased hyperactivated B cells and allo- and autoantibody titers.[5,6,8,12] After HCT, a unique combination of extrinsic factors including alloantigens and cytokines results in high potential for altered B- and T-cell homeostasis.[13,14] High B-cell activating factor (BAFF) is found in patients and has been shown to associate with activation and survival of aberrantly

Submitted 4 May 2017; accepted 24 August 2017. Prepublished online as *Blood* First Edition paper, 29 August 2017; DOI 10.1182/blood-2017-05-782466.

*J.C.P. and W.J. contributed equally to this manuscript and are joint first authors.

The online version of this article contains a data supplement.

There is an Inside *Blood* Commentary on this article in this issue.

The publication costs of this article were defrayed in part by page charge payment. Therefore, and solely to indicate this fact, this article is hereby marked "advertisement" in accordance with 18 USC section 1734.

activated B cells.[5,15] Compared with B cells from non-cGVHD patients, cGVHD B cells are activated via extracellular signal-regulated kinase (ERK) and AKT.[5] Total numbers of $CD27^+$ B cells remain persistently low after HCT.[16] cGVHD B cells are both paradoxically responsive to recipient antigens[17-19] and dysfunctional. Rare $CD27^+$ cells circulating in cGVHD patients constitutively produce immunoglobulin G (IgG), but are not typical "memory" B cells.[5] cGVHD patients are notoriously unable to combat encapsulated organisms or mount proper IgG recall responses.[20-22] Increased immature transitional-like CD21Lo B cells and a paucity of IgD^+CD27^+ "memory" B cells associate with increased infection rates in cGVHD.[23,24] Thus, constitutive B-cell activation in cGVHD may preclude functional B-cell maturation.

In cGVHD patients, heightened BCR responses and greater BAFF dependence for survival are functional properties shared with marginal zone (MZ) B cells.[5,6,25-27] Activation through the NOTCH2 receptor[28,29] and the level of BCR ligation are pivotal for MZ vs follicular B-cell fate in mice.[30,31] Notch ligands augment normal mouse BCR or CD40 responses to relatively high amounts of surrogate antigen or ligand.[32] T-cell alloreactivity after HCT is driven by NOTCH ligand in secondary lymphoid organs,[33] but whether B cells after HCT are aberrantly activated via the NOTCH pathway remains unknown. Given the well-defined role of NOTCH2 in the fate of immature-transitional B cells in both mice[29] and humans,[28] we hypothesized that NOTCH2 is aberrantly activated in cGVHD.

Using a human B-cell assay system, we discovered that B-cell hyperactivation in cGVHD is rooted in synergistic NOTCH2-BCR signaling. We also found that alterations in IRF4 and IRF8 are associated with NOTCH2 expression and hyperresponsiveness. Capitalizing on the pharmacological effect of all-*trans* retinoic acid (ATRA) on *IRF4* expression levels, we showed a mechanistic link between IRF4 and NOTCH2 that enabled reversal of the abnormal response of cGVHD B cells. NOTCH2-BCR axis blockade with ATRA also led to expression of *TLR9* and *PAX5*, indicating movement toward a B-cell maturation pathway.[34-36]

Table 1. Patients used in this study

Characteristic	No cGVHD, n = 13	Active cGVHD, n = 17	*P*
Median age (range), y	51 (29-73)	49 (22-69)	.57
Sex, females, no. (%)	5 (42)	5 (29)	.71
Median time after transplant (range), mo	43 (12-81)	45 (12-114)	.71
Conditioning regimen (%)			.71
Myeloablative	6 (46)	10 (59)	
Nonmyeloablative	7 (54)	7 (41)	
Source of graft (%)			1
Peripheral blood	10 (77)	13 (76)	
Bone marrow	3 (23)	4 (24)	
HLA matching (%)			.72
Matched, unrelated	7 (54)	8 (47)	
Matched, related	6 (46)	7 (41)	
Mismatched	0 (0)	2 (12)	
Immunosuppressive treatment (%)			<.0001
Prednisone <0.5 mg/kg	1 (8)	10 (59)	
MMF	0 (0)	1 (6)	
Tacrolimus	1 (8)	7 (41)	
Rapamycin	0 (0)	1 (6)	
Initial disease (%)			.41
AML/AML from MDS	4 (31)	5 (29)	
ALL	0 (0)	2 (12)	
CML	0 (0)	1 (6)	
CLL	2 (15)	1 (6)	
MDS	3 (23)	3 (18)	
NHL	1 (8)	2 (12)	
MM	1 (8)	0 (0)	
AA	2 (15)	0 (0)	
Other	0 (0)	3 (18)	

All patients were consented, all samples were obtained, and all studies were approved under the institutional review board protocols of Duke University, the National Institutes of Health, and the Dana-Farber Cancer Institute. Statistical comparisons between groups were performed using the Fisher exact test.

AA, aplastic anemia; ALL, acute lymphoblastic leukemia; AML, acute myeloid leukemia; CLL, chronic lymphocytic leukemia; CML, chronic myeloid leukemia; MDS, myelodysplastic syndrome; MM, multiple myeloma; MMF, mycophenolate mofetil.

Methods

Patient and healthy donor samples

Viably frozen peripheral blood mononuclear cells (PBMCs) from HCT patients were obtained with institutional review board protocols from Duke University, the National Cancer Institute (NIH), and the Dana-Farber Cancer Institute. Patient characteristics are described in Table 1 and supplemental Table 1 (available on the *Blood* Web site). Healthy donor PBMCs were obtained from Gulf Coast Regional Blood Center.

In vitro assays

B cells were purified using Human B Cell Isolation kits (Miltenyi Biotec). For NOTCH ligand stimulation, B cells were incubated on OP9-DL1 cells (kindly provided by Yuan Zhuang, Duke University, Durham, NC). B cells were B-cell receptor (BCR)-stimulated with anti-human IgM antibody (Ab) used as surrogate antigen plus or minus pan-NOTCH inhibition with 10 μM N-[N-(3,5-Difluorophenacetyl)-L-alanyl]-S-phenylglycine t-butyl ester (DAPT). To specifically inhibit NOTCH2 activation, the anti-NOTCH2 monoclonal Ab (mAb)[37] was used at 1 μg/mL vs 1 μg/mL mouse IgG2a anti-ragweed mAb[37] isotype control. We used 100 nM ATRA vs dimethyl sulfoxide (DMSO) as vehicle control, added 30 minutes before anti-IgM.

Flow cytometry

All Abs are listed in supplemental Methods. For intracellular flow cytometry, B cells were first stained for surface antigens and for live/dead cells before fixation and permeabilization.

Quantitative PCR

B cells were cultured for 24 hours plus or minus anti-IgM at the indicated doses, plus or minus ATRA, before harvest, total RNA isolation, and complementary DNA (cDNA) generation. Quantitative PCR (qPCR) was performed with the Applied Biosystems StepOne Plus System (Thermo Fisher Scientific) and Bio-Rad iTaq Universal SYBR Green Supermix.

NanoString and RNA-Seq analyses

Anti-N2 or isotype control mAbs (1 μg/mL) were added to B cells on OP9-DL1 feeder cell monolayers. After 30 minutes, anti-IgM was added. Twenty-four hours later, B cells were purified from the feeder cells via human CD19 microbeads (Miltenyi Biotec). B-cell total RNA was isolated by the RNeasy Plus kit. RNA-sequencing (RNA-Seq) data sets lacked detectable expression of genes characteristic of other leukocyte or precursor lineages, demonstrating high B-cell purity. NanoString gene-expression profiling of RNA samples was assessed via the nCounter Pan-Cancer Pathways Panel representing known NOTCH pathway genes. For RNA-Seq, RNA was subjected to Illumina HiSeq 125-bp paired-end sequencing.

High-throughput sequencing of *IGHV* genes

cDNA was amplified with the Invitrogen Superscript Platinum III Taq Hi-Fidelity RT-PCR kit. Primers for framework region 2 (FR2) of the immunoglobulin heavy-chain variable region (*IGHV*) genes and a common *IGH* joining (*J*) gene, were used for amplification.[38]

Further details are available in the supplemental Methods.

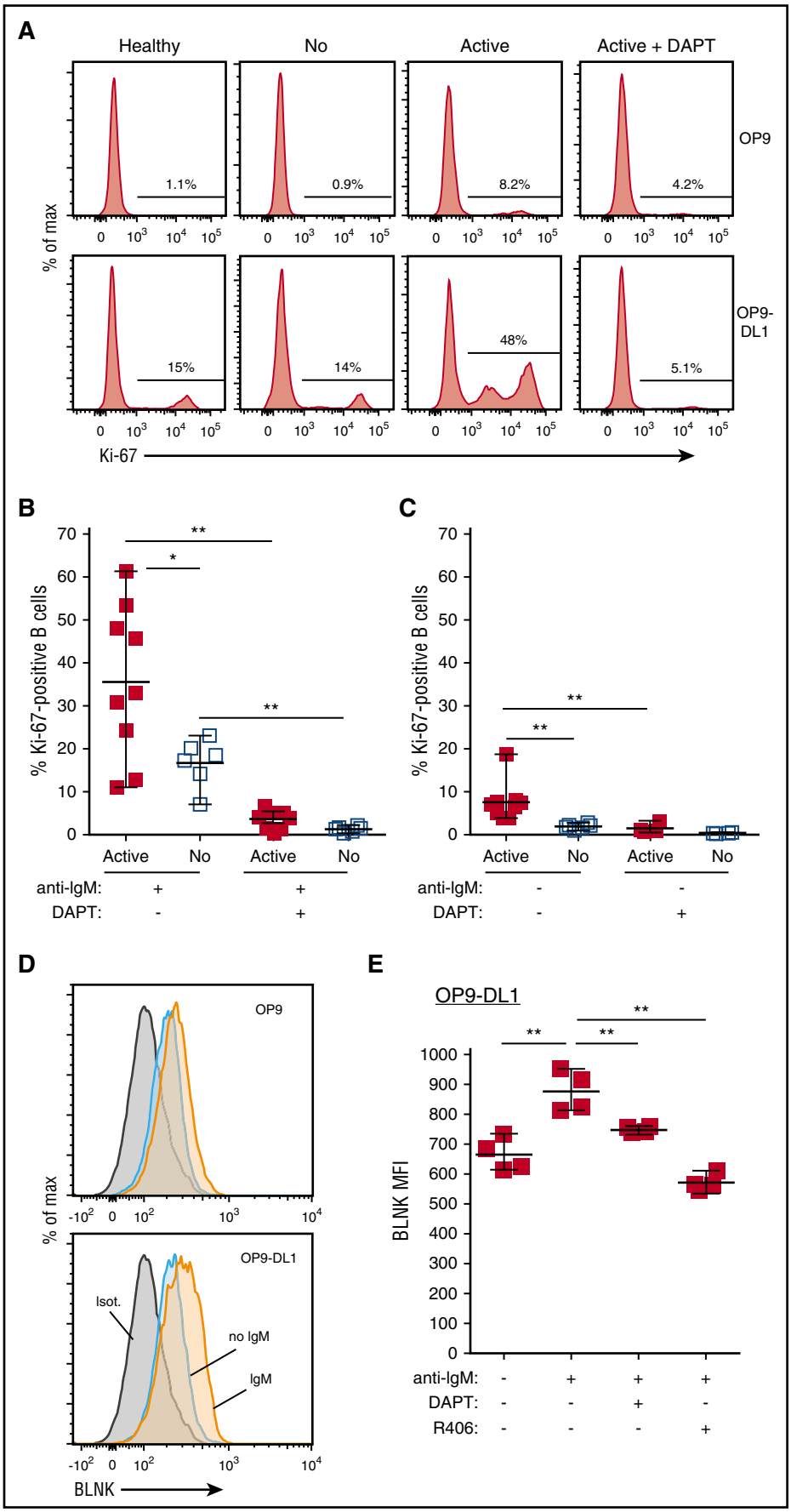

Figure 1. NOTCH2 ligation heightens ex vivo active cGVHD B-cell responses to minimal BCR engagement by surrogate antigen. B cells were magnetically purified to >95% from viably frozen PBMCs from HCT patients who at the time of sample collection had active cGVHD (Active; n = 9) or no cGVHD (No; n = 6). After plating B cells onto OP9 stromal cell monolayers or OP9-DL1 cells that express the NOTCH ligand DLL1, cultures were either treated with the γ-secretase inhibitor DAPT (10 μM in DMSO) to block Notch activation, or with DMSO alone. After 30 minutes, agonistic anti-IgM Ab was added to the appropriate wells at a concentration of 0.625 μg/mL. The cells were cultured for 72 hours, harvested, and flow cytometry analysis performed to assess Ki-67 expression. (A) Representative flow cytometry histograms for Ki-67 expression are shown for healthy donor (Healthy), no cGVHD (No), or active cGVHD (Active) donor B cells cultured in the presence of 0.625 μg/mL anti-IgM and plated on OP9 parental cells (top panels) or OP9-DL1 cells (bottom panels). The effect of DAPT treatment on active cGVHD B cells is also shown (right panels). (B-C) Frequency of Ki-67$^+$ B cells for all patients assessed in each group where the B cells were stimulated with 0.625 μg/mL anti-IgM (B) or were not stimulated through the BCR (C). *P* values were determined using a nonpaired Student *t* test for intergroup comparisons, and paired Student *t* test for same group comparisons. (D) Representative flow cytometry histograms showing BLNK expression as assessed by intracellular flow cytometry in B cells from active cGVHD patients stimulated as described for panel A, with plating on OP9 cells or OP9-DL1 cells. (E) Median fluorescence intensity (MFI) expression for BLNK in B cells from n = 4 active cGVHD patients stimulated as described for panel A and cultured on OP9-DL1 cells. In some cultures, DAPT (10 μM) was added to inhibit NOTCH activation, or R406 (0.1 μM) was added to inhibit SYK. DMSO alone used as the vehicle control in parallel. *P* values were determined using a paired Student *t* test.

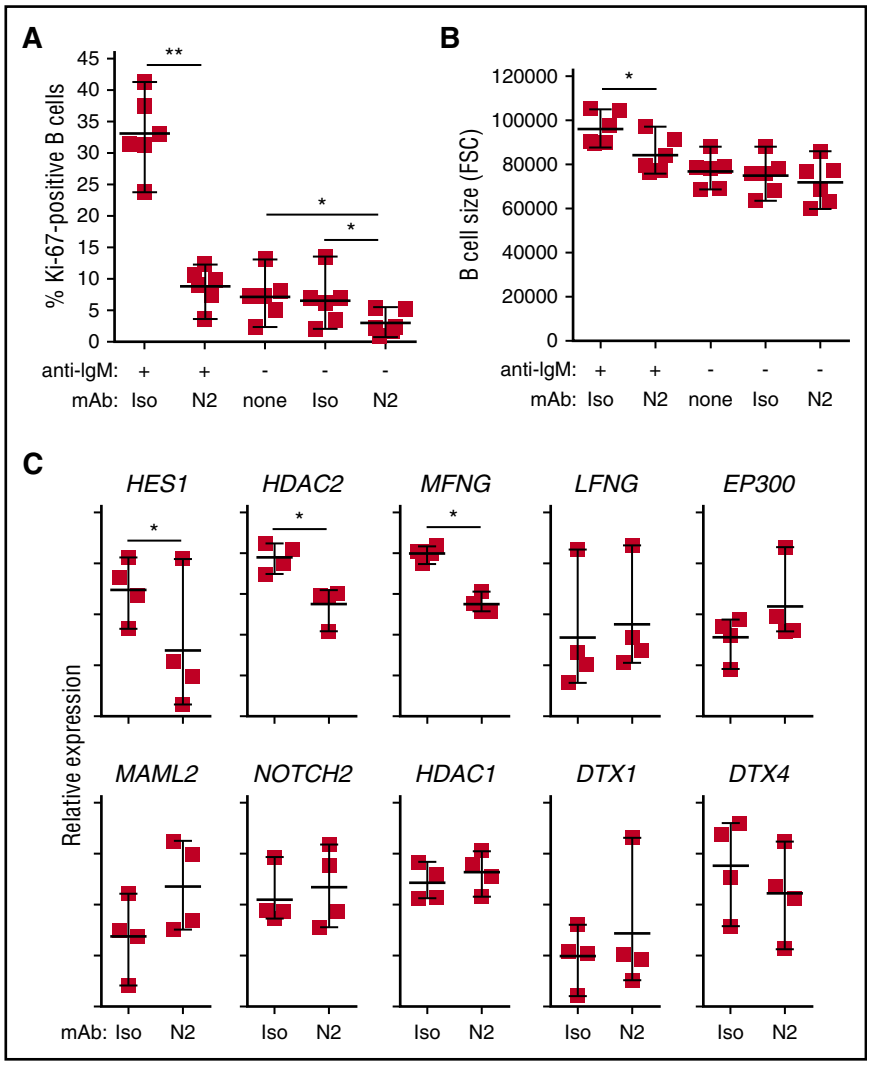

Figure 2. Hyperactivation of active cGVHD patient B cells to NOTCH ligand and anti-IgM is NOTCH2-dependent. (A-B) Anti-N2 mAb (N2) or ragweed isotype control mAb (Iso) were diluted in medium and added to 96-well plates containing OP9-DL1 feeder cell monolayers to achieve a final concentration of 1 μg/mL. B cells purified from viably frozen PBMCs of active cGVHD patients (n = 6) were then added to the plates. Following an initial culture period of 30 minutes, agonistic anti-IgM Ab was added to the appropriate wells at a final concentration of 0.625 μg/mL. The cells were cultured for 72 hours, harvested, and flow cytometry analysis performed to assess Ki-67 expression (A), and relative cell size by forward scatter (FSC) (B). *P* values were determined using a paired Student *t* test (**P* < .05; ***P* < .01). (C) NOTCH-BCR stimulation with or without specific NOTCH2 blockade with anti-N2, as described in panels A and B. The cells were cultured for 24 hours, the B cells purified away from the feeder cells using magnetic microbeads, and RNA isolated. B-cell RNA was then subjected in NanoString gene-expression profiling to assess differences in NOTCH pathway-regulated genes between groups. Data points represent NanoString nCounter target count number of individual samples for each gene, graphed on a relative scale. Statistical analysis comparing the anti-N2– and isotype control–treated groups was performed using a paired, negative binomial test (**P* < .05).

Results

Increased NOTCH activation heightens BCR responsiveness of cGVHD patient B cells

Thirty samples from HCT patients with or without active cGVHD were studied (Table 1; supplemental Table 1). At the time of sample acquisition, patients were on ≤0.5 mg/kg of steroids, were >12 months post-HCT, and had not received B-cell depletion or modulating therapies within 3 years.

To examine the effect of NOTCH ligand activation on BCR-stimulated B cells from cGVHD patients, we first tested whether NOTCH activation decreased the response threshold to low-dose surrogate antigen (anti-IgM) in our ex vivo assays. B cells from active cGVHD patients responded to 80-fold less anti-IgM than is required for optimal BCR activation when used alone.[6] Without NOTCH ligand (Figure 1A top panel), a small percentage of active cGVHD patient B cells became BCR-activated, whereas only about 1% of healthy or no cGVHD B cells became activated. With NOTCH ligand DLL1 (Figure 1A bottom panel), a higher proportion of B cells from active cGVHD patients was activated compared with B cells from healthy donors or patients without cGVHD. This response was blocked with γ-secretase inhibitor DAPT, which blocks proteolytic activation of NOTCH (Figure 1A right top and bottom panels). As in Figure 1B, after DLL1 and anti-IgM exposure, a significantly greater proportion of B cells from active cGVHD patients was activated vs B cells from patients without cGVHD. DAPT eliminated both high-level activation of cGVHD B cells and modest activation in B cells from patients without cGVHD, confirming the requirement for NOTCH (Figure 1B). Remarkably, even without ex vivo BCR stimulation, NOTCH activation induced modest and significant activation of cGVHD B cells compared with B cells from patients without cGVHD (Figure 1C), an effect also abolished by DAPT-mediated NOTCH blockade. These data suggest that constitutive BCR activation in vivo primes cGVHD B cells to respond through NOTCH.

We previously found that BLNK expression increases after BCR activation of healthy B cells and is constitutively increased in B cells from patients with active cGVHD.[6] BLNK protein increased in a NOTCH-BCR–dependent manner in active cGVHD B cells (Figure 1D-E). Pan-NOTCH (with DAPT) or BCR blockade (with Syk inhibitor, R406/fostamatinib) each reduced BLNK to similar levels of unstimulated B cells (Figure 1E). Thus, data suggest that the BCR pathway in active cGVHD B cells is in vivo–primed by NOTCH for immediate antigen responsiveness.

Table 2. NOTCH2 blockade alters the expression of diverse genes

Gene	Pathway/Function	log_2 fold change	Fold change	*P*	Adjusted *P*
DNASE1L3	Apoptosis/DNA hydrolysis	−2.50	−5.65	7.04×10^{-20}	9.07×10^{-16}
HES4	[NOTCH pathway]	−2.97	−7.86	2.79×10^{-17}	1.80×10^{-13}
CR2	BCR/Complement binding	−1.76	−3.38	2.70×10^{-16}	1.16×10^{-12}
*FOS**	Cell-cycle control/Transcription factor, MAPK pathway	1.55	2.93	1.37×10^{-9}	4.42×10^{-6}
CD300A	Immune response/Inhibitory receptor for phosphatidylserine	−1.80	−3.49	2.00×10^{-8}	3.70×10^{-5}
DTL	Cell-cycle control, DNA damage response/E3 ubiquitin ligase activity	−1.46	−2.74	1.45×10^{-8}	3.70×10^{-5}
FCRL4	B-cell receptor/Signal modulation/Marginal zone B cells	−1.59	−3.01	2.01×10^{-8}	3.70×10^{-5}
*MMP9**	Extracellular matrix organization/[NOTCH regulation reported]	1.77	3.40	2.90×10^{-8}	4.66×10^{-5}
IL12RB2	Immune response	−1.59	−3.01	1.91×10^{-7}	2.53×10^{-4}
*MACROD2**	Signal modulation/Wnt pathway	0.951	1.93	1.96×10^{-7}	2.53×10^{-4}
ABHD6	Signal modulation/GPCR signaling	−1.15	−2.21	5.56×10^{-7}	6.51×10^{-4}
CDC6	Cell-cycle control	−1.34	−2.52	6.26×10^{-7}	6.72×10^{-4}
CHI3L2	Cartilage biogenesis	−1.49	−2.82	9.30×10^{-7}	9.21×10^{-4}
*DUSP1**	Signal modulation/MAPK pathway/[NOTCH regulation reported]	1.21	2.31	1.61×10^{-6}	1.49×10^{-3}
*C11orf21**	(Unknown)	1.53	2.89	2.52×10^{-6}	2.15×10^{-3}
TFRC	Immune response/Iron metabolism	−1.04	−2.05	2.67×10^{-6}	2.15×10^{-3}
RHOBTB1	GTPase activity/GPCR signaling	−1.13	−2.19	6.94×10^{-6}	5.26×10^{-3}
*CD68**	Scavenger receptor	0.998	2.00	7.40×10^{-6}	5.29×10^{-3}
SLC19A1	Folate transport/Cell-cycle control	−1.09	−2.14	8.60×10^{-6}	5.83×10^{-3}
*CD14**	Immune response/LPS binding	1.51	2.84	1.14×10^{-5}	6.39×10^{-3}
DDN	Apoptosis	−1.50	−2.83	1.07×10^{-5}	6.39×10^{-3}
*MRC1**	Immune response/Mannose binding	1.56	2.95	1.12×10^{-5}	6.39×10^{-3}
*RSAD2**	Immune response/Antiviral response	1.33	2.51	1.02×10^{-5}	6.39×10^{-3}
*IFIT1**	Immune response/Antiviral response/RNA binding	1.11	2.17	1.46×10^{-5}	7.85×10^{-3}
*HMOX1**	Heme catabolism/NF-κB signaling	1.03	2.04	1.94×10^{-5}	.010
*SNX29P2**	(Unknown; pseudogene)	0.937	1.91	2.20×10^{-5}	.011
*PSTPIP1**	BCR/Immune response/Actin cytoskeleton	0.889	1.85	2.39×10^{-5}	.011
MACROD1	Signal modulation/Deacetylation of ADP ribose moieties	−1.01	−2.01	2.60×10^{-5}	.012
PPIF	Apoptosis/Protein folding	−0.896	−1.86	2.81×10^{-5}	.012
*NCF2**	Immune response/GPCR signaling	0.762	1.70	6.52×10^{-5}	.027
*TNFSF12**	Immune response/Apoptosis/[NOTCH regulation reported]	0.886	1.85	6.56×10^{-5}	.027
BIRC5	Apoptosis/Cell-cycle control/[NOTCH regulation reported]	−1.39	−2.61	7.24×10^{-5}	.027
CTPS1	Immune response/Nucleic acid biosynthesis, metabolism	−0.946	−1.93	7.04×10^{-5}	.027
FKBP4	Immune response/Protein folding, trafficking/[Negative regulator of IRF4]	−0.862	−1.82	6.84×10^{-5}	.027
SLC16A9	Metabolism/Membrane transport	−1.35	−2.55	8.87×10^{-5}	.033
*CARNS1**	Metabolism/Amino acid biosynthesis	1.25	2.37	9.51×10^{-5}	.033

NOTCH2 blockade alters the expression of diverse genes in NOTCH2/BCR-stimulated B cells from active cGVHD patients. RNA samples used in the NanoString analysis described in Figure 2C were also subjected to Illumina HiSeq 125-bp paired-end sequencing. Genes shown represent those significantly altered by NOTCH2 blockade ranked in order of significance based on the adjusted *P* value, determined as described in supplemental Methods. All genes with an adjusted *P* value of $<.05$ are shown.

GPCR, G-protein–coupled receptor; LPS, lipopolysaccharide; mRNA, messenger RNA; ncRNA, noncoding RNA.

Genes shown in bold are downregulated by NOTCH2 blockade.

*Genes upregulated by NOTCH2 blockade.

Table 2. (continued)

Gene	Pathway/Function	log_2 fold change	Fold change	*P*	Adjusted *P*
CDC25A	BCR/Cell-cycle control, DNA damage response/MAPK pathway	−1.24	−2.36	9.48×10^{-5}	.033
CYP2J2	Metabolism/Arachidonic acid metabolism	−1.37	−2.58	9.90×10^{-5}	.034
*ANPEP**	Metabolism/Golgi protein transport	1.36	2.57	1.19×10^{-4}	.035
*C5AR1**	Immune response/Complement binding	1.34	2.53	1.22×10^{-4}	.035
*CTSL1**	Immune response/Antigen processing and presentation	1.36	2.56	1.20×10^{-4}	.035
HNRNPAB	mRNA splicing	−0.750	−1.68	1.19×10^{-4}	.035
LCN10	Carrier protein activity	−0.859	−1.81	1.18×10^{-4}	.035
*MOV10**	Immune response/RNA helicase activity, mRNA processing	0.942	1.92	1.17×10^{-4}	.035
*PTRF**	Transcriptional regulation	1.27	2.41	1.13×10^{-4}	.035
ANKLE1	Endonuclease activity	−0.864	−1.82	1.35×10^{-4}	.037
*FCGBP**	Maintenance of mucosal integrity	1.35	2.55	1.37×10^{-4}	.037
*CORO2B**	Cytoskeletal reorganization	1.33	2.52	1.47×10^{-4}	.039
*IL8**	Immune response/Chemoattraction	1.29	2.45	1.49×10^{-4}	.039
MYBL2	Cell-cycle control	−1.01	−2.02	1.52×10^{-4}	.039
IL6R	Immune response/Plasma cell development/[NOTCH regulation reported]	−0.713	−1.64	1.61×10^{-4}	.041
*DAB2**	Immune response/Signal modulation/Endocytosis/Wnt pathway	1.27	2.42	1.78×10^{-4}	.043
*LRRC37A4P**	(Unknown; pseudogene)	1.33	2.51	1.83×10^{-4}	.043
SLC16A1	Metabolism/Membrane transport	−0.991	−1.99	1.72×10^{-4}	.043
SRM	Metabolism/Spermidine biosynthesis/Amino acid metabolism	−0.709	−1.63	1.85×10^{-4}	.043
TTLL12	Cell-cycle control/Cytoskeletal reorganization	−0.746	−1.68	1.82×10^{-4}	.043
SKA3	Cell-cycle control/Cytoskeletal reorganization	−1.26	−2.39	2.02×10^{-4}	.045
TOMM40	Metabolism/Mitochondrial membrane transport	−0.680	−1.60	2.02×10^{-4}	.045
MEST	Wnt pathway/Genetic imprinting	−0.998	−2.00	2.10×10^{-4}	.046
ORC6	Cell-cycle control	−1.07	−2.10	2.25×10^{-4}	.047
RGS16	Immune response/GPCR signaling	−0.934	−1.91	2.21×10^{-4}	.047
PAICS	Metabolism/Purine metabolism	−0.715	−1.64	2.38×10^{-4}	.049
UBE2C	Cell-cycle control/E2 ubiquitin ligase activity	−1.30	−2.46	2.36×10^{-4}	.049
*LOC100506123**	(Unknown; ncRNA class gene)	1.28	2.42	2.48×10^{-4}	.049
TYMS	Metabolism/Pyrimidine metabolism	−0.999	−2.00	2.47×10^{-4}	.049

NOTCH2 blockade alters the expression of diverse genes in NOTCH2/BCR-stimulated B cells from active cGVHD patients. RNA samples used in the NanoString analysis described in Figure 2C were also subjected to Illumina HiSeq 125-bp paired-end sequencing. Genes shown represent those significantly altered by NOTCH2 blockade ranked in order of significance based on the adjusted *P* value, determined as described in supplemental Methods. All genes with an adjusted *P* value of $<.05$ are shown.

GPCR, G-protein–coupled receptor; LPS, lipopolysaccharide; mRNA, messenger RNA; ncRNA, noncoding RNA.

Genes shown in bold are downregulated by NOTCH2 blockade.

*Genes upregulated by NOTCH2 blockade.

Table 3. GO: Biological process classification of genes within the NOTCH, BCR, and cell-cycle–signaling cascades in cGVHD B cells after NOTCH2 blockade

Pathway	Gene identifier	Name/Aliases
Notch signaling	***HES4***	Hes family BHLH transcription factor 4
	*MMP9**	Matrix metalloproteinase 9
	*DUSP1**	Dual-specificity phosphatase 1
	*TNFSF12**	Tumor necrosis factor superfamily member 12; *TWEAK*
	BIRC5†	Baculoviral IAP repeat containing 5
	IL6R	Interleukin 6 receptor; CD126 antigen
BCR signaling	*FOS**†	Cellular oncogene C-Fos
	CR2	Complement component 3d receptor 2; CD21 antigen
	FCRL4	Fc receptor-like 4; *IRTA1*
	*PSTPIP1**	Proline-serine-threonine phosphatase-interacting protein 1
	CDC25A†	Cell division cycle 25A
Cell cycle	*FOS**†	Cellular oncogene C-Fos
	DTL	Denticleless E3 ubiquitin protein ligase homolog
	CDC6	Cell division cycle 6
	SLC19A1	Solute carrier family 19 member 1
	BIRC5†	Baculoviral IAP repeat containing 5
	CDC25A†	Cell division cycle 25A
	MYBL2	MYB proto-oncogene–like 2
	TTLL12	Tubulin tyrosine ligase–like 12
	SKA3	Spindle and kinetochore–associated complex subunit 3
	ORC6	Origin recognition complex subunit 6
	UBE2C	Ubiquitin-conjugating enzyme E2 C

BHLH, basic helix loop helix; IAP, inhibitor of apoptosis.
Genes shown in bold are downregulated by NOTCH2 blockade.
*Genes upregulated by NOTCH2 blockade.
†Genes categorized into >1 signaling pathway.

NOTCH-BCR activation of B cells from cGVHD patients relies on NOTCH2

NOTCH2 is the dominant NOTCH receptor expressed by B cells and is essential for MZ B-cell development.[28,29] Because DAPT is a pan-NOTCH inhibitor, we tested whether NOTCH2 is specifically responsible for the heightened activation of cGVHD B cells. For this, we used an antagonistic anti-NOTCH2 mAb that specifically inhibits NOTCH2 activation by DLL1.[37] This mAb, called "anti-N2" herein (also known as anti–negative regulatory region 2 [anti-NRR2][37]), binds and stabilizes the NOTCH2 NRR, preventing activation. As shown in Figure 2A, anti-N2 effectively suppressed cGVHD B-cell responses to NOTCH-BCR stimulation. Anti-N2 also significantly blocked the modest response to NOTCH ligand alone. Anti-N2 conferred significantly decreased cell size after NOTCH2-BCR stimulation, suggesting prevention of B-cell blast development (Figure 2B). NOTCH blockade did not cause B-cell death because B-cell numbers were not different after anti-N2 compared with isotype control mAbs or DAPT (data not shown). To qualitatively assess how anti-N2 affected cGVHD B-cell activation, we analyzed genes associated with NOTCH using a NanoString expression-profiling platform. As shown in Figure 2C, anti-N2 significantly and selectively reduced expression of *HES1*, *HDAC2*, and *MFNG*, whereas other genes in the NOTCH pathway remained unaffected. Together, these data demonstrate that NOTCH-BCR hyperresponsiveness in cGVHD B cells requires NOTCH2.

Downstream effectors of NOTCH2 in B cells remain largely unknown[39] and have not been studied in cGVHD. Anti-N2 blocks proteolysis and release of the NOTCH2 intracellular domain, effectively blocking NOTCH2-induced transcription.[37] We thus used RNA-Seq to identify additional gene alterations in BCR-NOTCH–stimulated cGVHD B cells caused by NOTCH2 blockade via paired comparison of 4 active cGVHD patient B-cell samples treated with anti-N2 vs isotype control mAb. A total of 12 880 genes were expressed above background in the RNA-Seq analysis. Of these, NOTCH2 blockade led to the differential expression of 65 genes with an adjusted P value of $<.05$ (Benjamini-Hochberg method calculation to account for multiple comparisons[40]; Table 2), and 1478 genes having an overall P value of $<.05$ (supplemental Table 2). Strikingly, NOTCH2 blockade on cGVHD B cells was not globally suppressive, as both increased and decreased gene-expression changes occurred (42% and 58%, respectively; Table 2). Kyoto Encyclopedia of Genes and Genomes pathways analysis of the RNA-Seq data showed that the cell-cycle pathway and multiple metabolic pathways were downregulated by NOTCH2 blockade (supplemental Figure 1A; supplemental Table 3). Other important pathways were upregulated, including the MAPK and BCR pathways (supplemental Figure 1B; supplemental Table 3). Importantly, apoptosis pathways were not altered by NOTCH2 blockade (supplemental Table 3), further suggesting no negative impact on B-cell survival. Gene Ontology (GO): Biological Process (www.geneontology.org) classification of the 65 genes in Table 2 identified important mediators of immune responses, including BCR signaling, NOTCH signaling, and cell-cycle progression (Table 3). Notably, genes encoding proteins critical to MZ-like B-cell development and function, *CR2* (*CD21*) and *FCRL4* (*IRTA1*), were significantly decreased by NOTCH2 blockade. By contrast, anti-N2 enhanced genes of known importance for follicular B cells, including *DUSP1*, *TNFSF12*, and *FOS*. Putative NOTCH pathway genes identified in the RNA-Seq analysis were in agreement with the NanoString findings, except that *LFNG* reached a significant P value by RNA-Seq only (supplemental Table 4). Altered *MFNG* and *LFNG* expression is intriguing because these *FRINGE* glycosyltransferases modify the extracellular domains of NOTCH receptors, altering their affinity for NOTCH ligands, including NOTCH2-DLL1 pairing during MZ B-cell development.[41] Our results reveal the importance of NOTCH2 activation in cGVHD B cells, and implicate candidate genes essential to this process.

NOTCH-BCR activation leads to persistent surface expression of NOTCH2 on cGVHD B cells

We next examined whether BCR activation affected NOTCH2 expression in cGVHD. Freshly isolated B cells from active cGVHD patients, patients without cGVHD, and healthy donors all expressed similar surface NOTCH2 (supplemental Figure 2). With continuous NOTCH ligand and anti-IgM stimulation, however, B cells from active cGVHD patients maintained significantly higher NOTCH2 surface expression (Figure 3A-B), similar to expression found without NOTCH ligand (no DLL1; data not shown). NOTCH2 expression on active cGVHD B cells was significantly reduced with DAPT (Figure 3A-B). On healthy B cells, NOTCH2 was expressed at increasing levels on the surface with increasing doses of anti-IgM (Figure 3C left panel), whereas in the presence of NOTCH ligand, NOTCH2 surface expression was not maintained (Figure 3C right panel). Thus, persistent NOTCH2 expression by active cGVHD B cells likely reflects a positive feedback-activation loop dependent on both NOTCH2 and the BCR.

Skewing of the BCR repertoire could potentially cause enhanced surrogate antigen sensitivity. To address this, we used high-throughput sequencing of the *IGHV* complementarity-determining region 3 (CDR3) repertoire in various BCR-activated $CD27^+$ and $CD27^-$ B-cell subsets.[14] This limited analysis revealed similar usage frequency of the majority of *IGHV* genes between active cGVHD patients and healthy donors, as

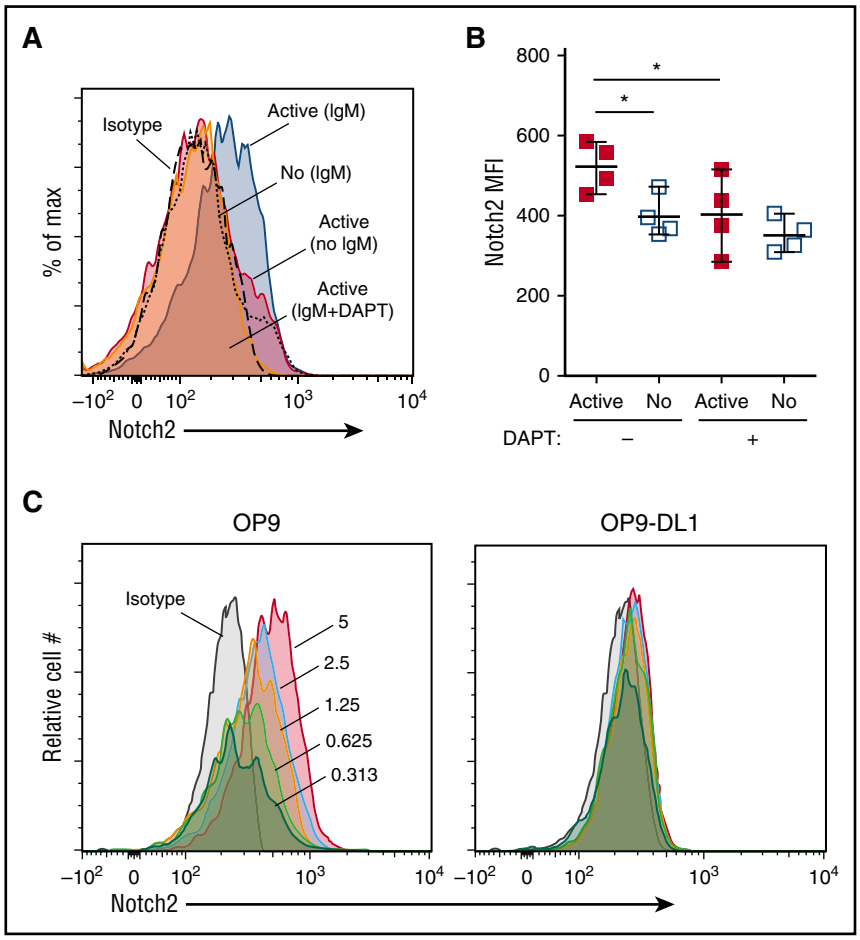

Figure 3. NOTCH2 expression is maintained on active cGVHD B cells in the presence of NOTCH ligand and BCR stimulation. (A-B) B cells were purified from viably frozen PBMCs of HCT patients with active cGVHD (Active, n = 4) or no cGVHD (No, n = 4) and plated in medium onto OP9-DL1 feeder cell monolayers. In some wells, the γ-secretase inhibitor DAPT was added for a final concentration of 10 μM, with DMSO alone used as the vehicle control in parallel. Following an initial culture period of 30 minutes, agonistic anti-IgM Ab was then added to the appropriate wells at a concentration of 0.625 μg/mL. The cells were cultured for 72 hours, harvested, and flow cytometry analysis performed to assess NOTCH2 surface expression on $CD19^+$ B cells. (A) Representative histogram overlay showing relative NOTCH2 expression between patient groups and activation conditions (as indicated). (B) MFI values for all patients assessed under conditions of anti-IgM stimulation, either without or with DAPT. (C) B cells were purified from viably frozen PBMCs from healthy donors and then plated onto monolayers of parental OP9 cells or OP9-DL1 cells, with various concentrations of anti-IgM Ab (micrograms per milliliter, indicated by numbers in the OP9 histogram overlay). Following a culture period of 72 hours, the cells were harvested and analysis of NOTCH2 expression on $CD19^+$ cells was performed by flow cytometry. In panel B, *P* values were determined using a nonpaired Student *t* test for Active vs No comparison, and a paired Student *t* test for Active (no DAPT) vs Active (DAPT) comparison. $^*P < .05$.

well as between each cell subset examined (supplemental Figure 3). Consistent with this, there were no differences in cGVHD B-cell subset CDR3 Shannon entropy or mutational scores (data not shown). Thus, a major skewing of the BCR repertoire unlikely explains NOTCH2-BCR hyperresponsiveness of cGVHD B cells.

IRF4 and *IRF8* are altered in cGVHD B cells, especially after BCR engagement

Increased BCR signaling across various populations of B cells in cGVHD[6] suggested that additional intrinsic molecular alterations underlie their hyperactivated state. Because inducible deletion of the transcription factor *IRF4* in the B-cell lineage in mice leads to enhanced NOTCH2 expression,[42] we examined *IRF4* expression in cGVHD B cells. It has been hypothesized that BCR-signaling strength regulates IRF4 levels.[43] After BCR stimulation, *IRF4* transcripts were significantly lower in B cells from active cGVHD patients relative to B cells from patients with no cGVHD (Figure 4A), consistent with our previous finding in $CD27^+$ B cells.[6] Interestingly, at low-dose anti-IgM, B cells from patients without cGVHD had significantly increased *IRF4* expression compared with healthy B cells. Regardless, the significant *IRF4* decrease in B cells from HCT patients with cGVHD suggests a molecular link between this pivotal transcription factor and NOTCH2.

IRF8 attenuates BCR signaling in a fashion that antagonizes IRF4. A critical balance between IRF4 and IRF8 determines mouse B-cell fate after antigen encounter in vivo.[44] Thus, we also assessed *IRF8* compared with *IRF4* transcripts. Remarkably, *IRF8* expression was significantly increased in unstimulated B cells from both active cGVHD and no cGVHD patient groups relative to healthy donors (Figure 4B). This indicates a fundamental change in *IRF8* expression after HCT. Because IRF8 overexpression is associated with B-cell anergy,[45] this enhancement in *IRF8* may contribute to B-cell tolerance in the HCT setting. Upon BCR engagement at both low and high doses of anti-IgM, *IRF8* levels were significantly reduced in each of the 3 groups relative to unstimulated B cells ($P < .05$ for active cGVHD; $P < .01$ for no cGVHD, healthy donors). Importantly, *IRF8* transcripts remained significantly higher in B cells from active cGVHD patients compared with healthy donors at each anti-IgM concentration, whereas *IRF8* transcripts remained significantly higher in B cells from patients without cGVHD compared with healthy donors only at the higher dose (Figure 4B). We found the *IRF4*-to-*IRF8* ratio in resting B cells was significantly lower for both HCT patient groups compared with healthy donors (Figure 4C). Remarkably, only B cells from active cGVHD patients maintained a significantly reduced median *IRF4*-to-*IRF8* ratio after stimulation with low or higher dose surrogate antigen (Figure 4C). Thus, because functional humoral immune responses are known to rely on an intricate balance in the relative expression of *IRF4* and *IRF8* during various stages of B-cell development and activation,[43,44,46-48] our findings suggest that these transcription factors may represent a pivotal B-cell maturation checkpoint after HCT.

The vitamin A metabolite ATRA increases *IRF4* expression in normal human B cells stimulated with cytosine guanine dinucleotide (CpG).[49] Thus, we tested whether ATRA enhances the blunted *IRF4* expression and increases the *IRF4*-to-*IRF8* ratio in BCR-stimulated

Figure 4. Altered *IRF4* and *IRF8* gene expression in B cells from active cGVHD patients, with normalization by ATRA. B cells from HCT patients with active cGVHD vs no cGVHD (n = 6), or from healthy donors (n = 6) were cultured in medium alone, or with low-dose (0.625 μg/mL) or high-dose (5 μg/mL) concentrations of anti-IgM for 24 hours. The B cells were then harvested, total RNA isolated, and real-time qPCR analysis performed to assess the abundance of *IRF4* and *IRF8* transcripts. The relative expression level shown for each gene is normalized to the median value for healthy donors with no anti-IgM stimulation, represented as a value of 1. (A) *IRF4* and (B) *IRF8* mRNA levels in each of the 3 sample groups with and without BCR stimulation. (C) Normalized *IRF4* and *IRF8* mRNA expressed as the ratio of *IRF4* to that of *IRF8* transcripts (*IRF4*-to-*IRF8*). *P* values were determined using a nonpaired Student *t* test (**P* < .05; ***P* < .01). (D) B cells from HCT patients with active cGVHD (n = 6) were cultured with ATRA (0.1 μM) or vehicle alone, followed 30 minutes later by the addition of 0.625 μg/mL anti-IgM. Following a 24-hour culture period, the B cells were then harvested, total RNA isolated, and real-time qPCR analysis performed to determine relative *IRF4* and *IRF8* expression, and the *IRF4*-to-*IRF8* ratio, as described for panels B and C. (E) B cells from HCT patients with active cGVHD (n = 4-6) were plated onto OP9-DL1 monolayers in the presence of ATRA (0.1 μM) or vehicle alone. Following an initial culture period of 30 minutes, agonistic anti-IgM Ab was then added to the appropriate wells at a final concentration of 0.625 μg/mL. The cells were cultured for 24 hours, harvested, and intracellular staining with flow cytometry analysis performed to assess IRF4 and IRF8 levels. For each protein, data represent the ratio of ATRA-treated B cells over vehicle-treated B cells, with the dashed line included for reference to a value of 1.0.

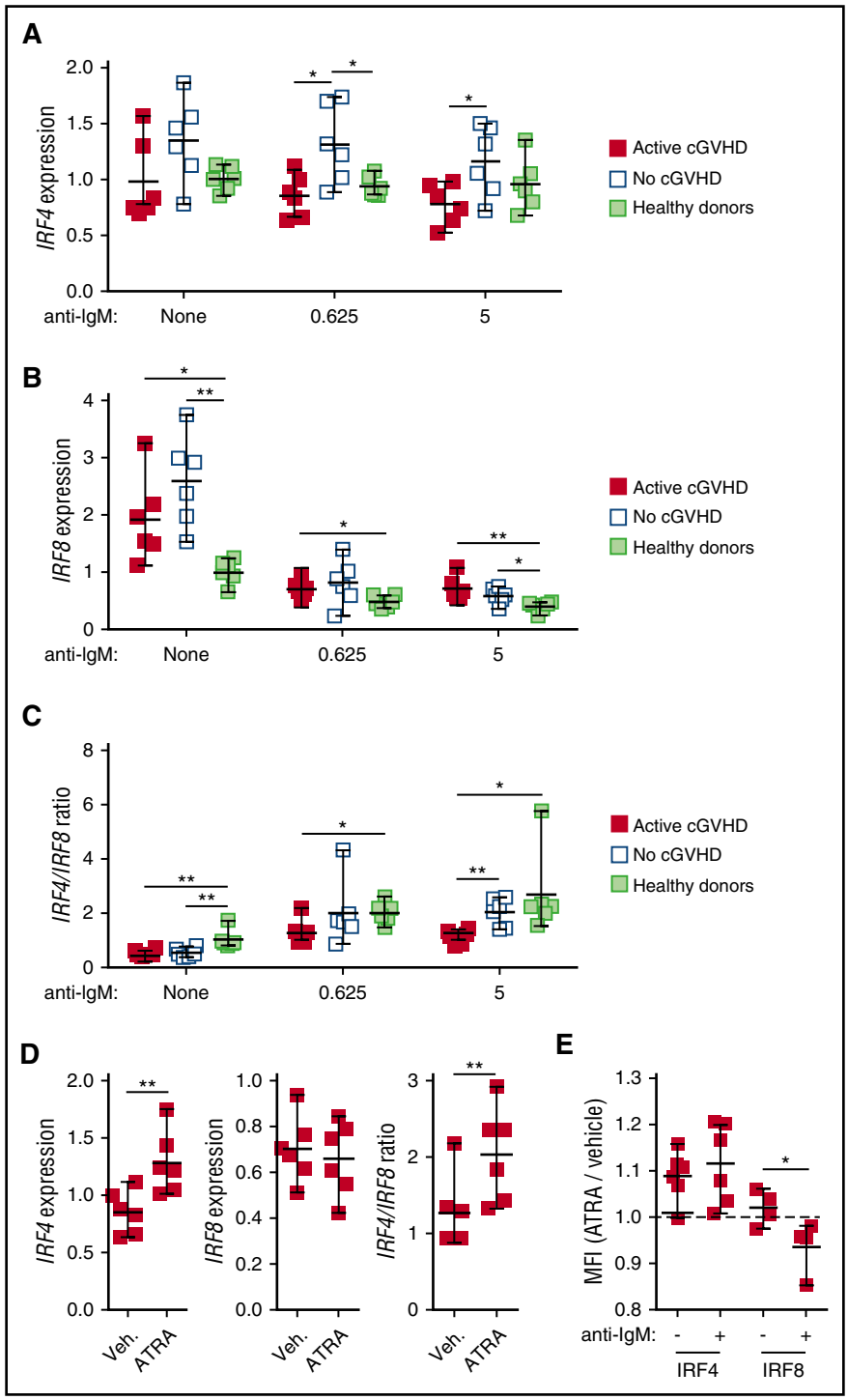

cGVHD B cells. ATRA treatment of cGVHD B cells during BCR activation significantly increased *IRF4* levels relative to vehicle (Figure 4D left panel). Although *IRF8* transcripts were not significantly altered by ATRA (Figure 4D middle panel), the effect of ATRA on *IRF4* expression conferred a significant increase in the *IRF4*-to-*IRF8* ratio (Figure 4D right panel). To confirm that ATRA also affected IRF4 and IRF8 at the protein level, even in the presence of NOTCH ligand, we performed intracellular staining and flow cytometry analysis. IRF4 protein levels increased with ATRA treatment above vehicle control (Figure 4E), in the presence or absence of BCR stimulation. Strikingly, ATRA treatment significantly reduced IRF8 protein levels with BCR stimulation (Figure 4E), demonstrating that IRF8 loss can also contribute to altered IRF4-to-IRF8 ratios in cGVHD B cells at the protein level.

ATRA alters the genetic maturation program of cGVHD B cells and restores CpG responsiveness

Foreign antigen-responsive, mature follicular B cells have a gene signature, which includes enhanced expression of *PAX5*[34,36] and

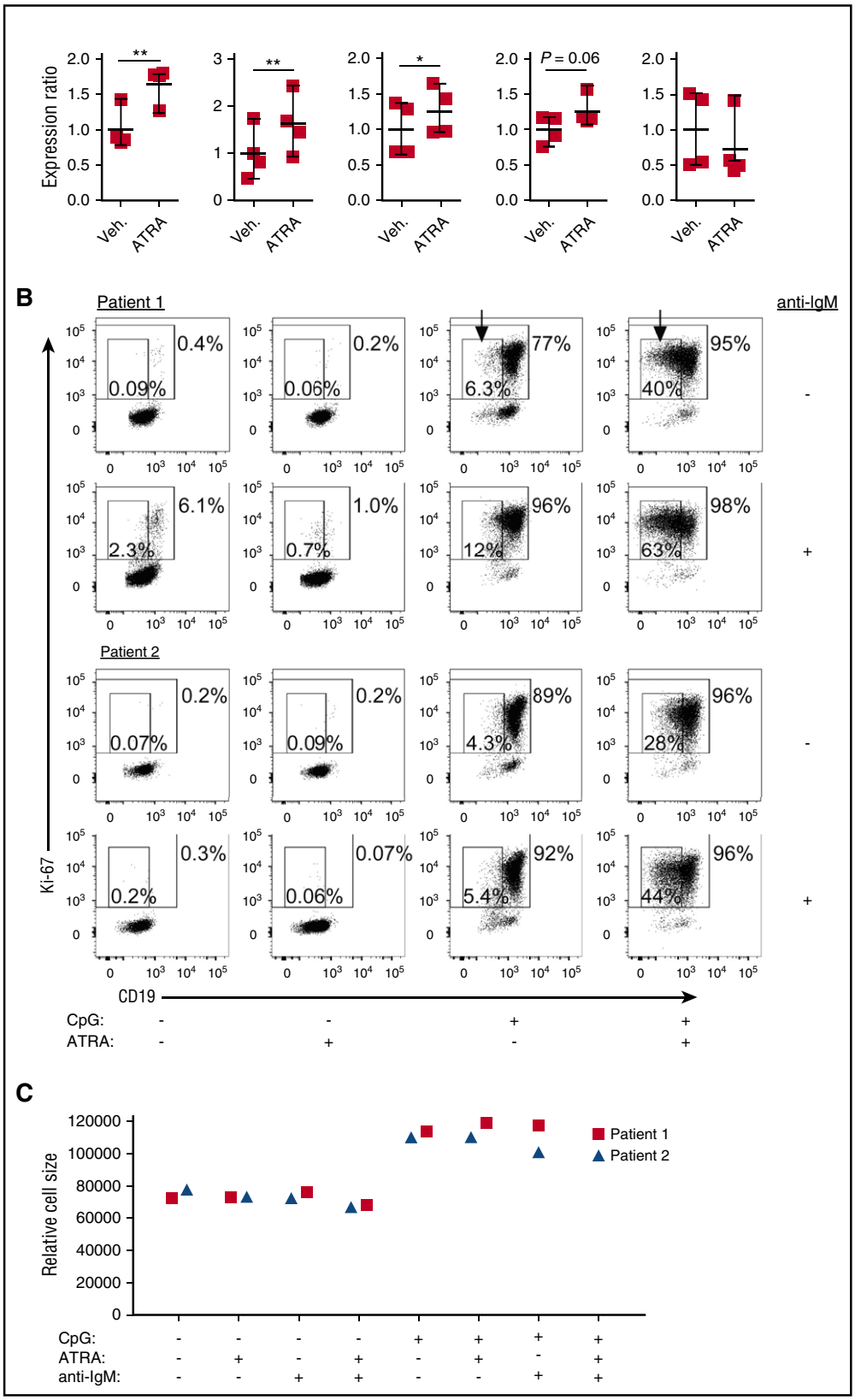

Figure 5. ATRA treatment of B cells from active cGVHD patients enhances genes involved in B-cell maturation. (A) B cells from active cGVHD patients (n = 4) were treated with ATRA (0.1 μM) or vehicle alone for 24 hours. The B cells were harvested, total RNA isolated, and real-time qPCR analysis performed to assess the expression levels of genes of interest. *P* values were determined using a paired Student *t* test (*$P < .05$; **$P < .01$). (B-C) Purified B cells from active cGVHD patients were plated in medium in the presence of ATRA (0.1 μM) or DMSO vehicle control. Following an initial culture period of 30 minutes, CpG (1 μg/mL) or anti-IgM Ab (0.625 μg/mL) were added alone or in combination. The cells were cultured for 72 hours, harvested, and flow cytometry analysis performed to assess Ki-67 and CD19 expression (B), as well as relative cell size by FSC (C). In panel B, the large gates with numbers outside indicate the frequency of Ki-67$^+$ B cells, and the small gates (arrows) with numbers inside represent the frequency of proliferating, CD19^{low} B cells.

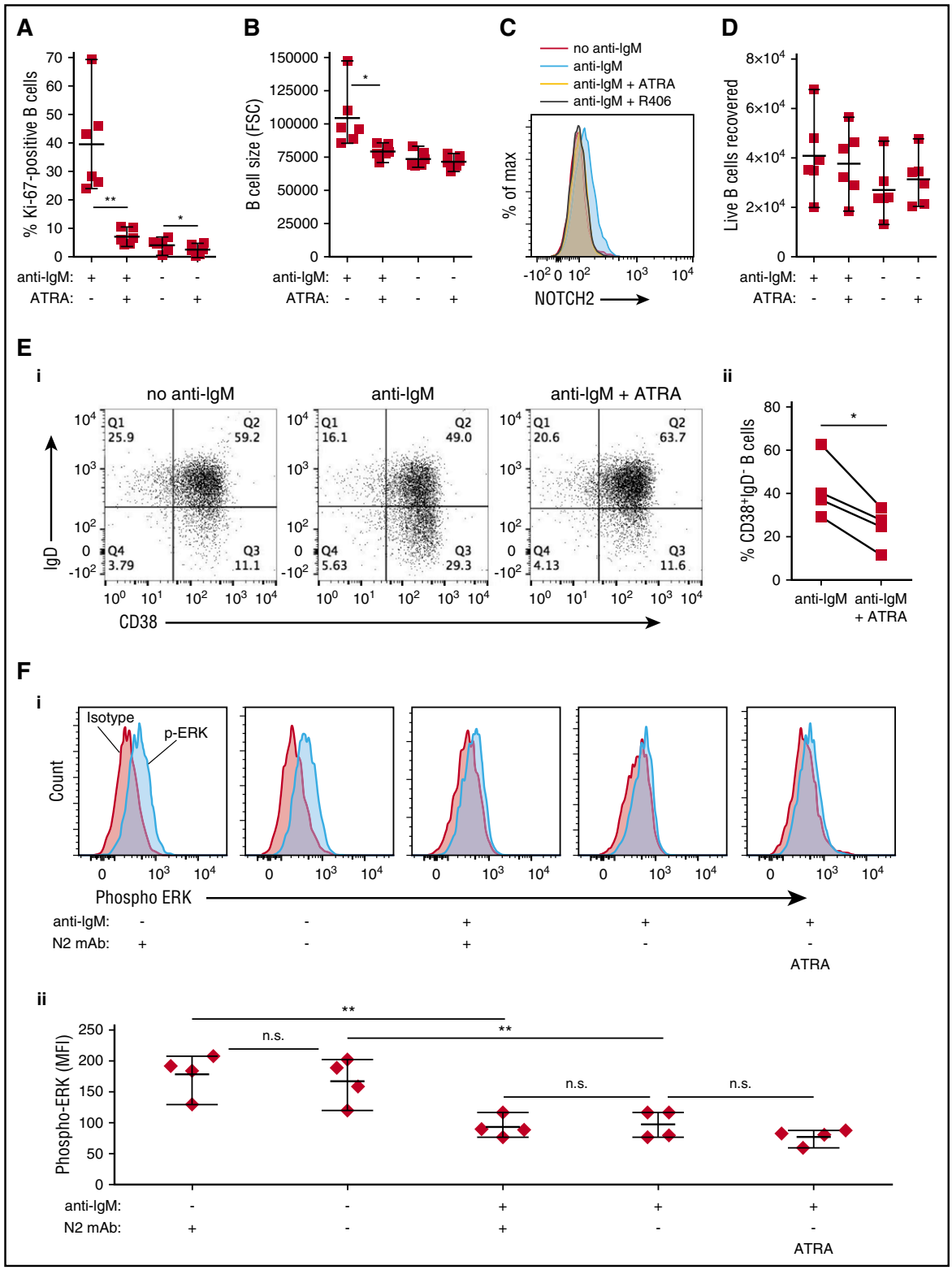

Figure 6. ATRA suppresses NOTCH2-BCR hyperresponsiveness of B cells from active cGVHD patients. (A-D) B cells from HCT patients with active cGVHD (n = 6) were plated in medium on monolayers of OP9-DL1 feeder cells and exposed to ATRA (0.1 μM) or vehicle alone. Following an initial culture period of 30 minutes, agonistic anti-IgM Ab was then added to the appropriate wells at a final concentration of 0.625 μg/mL. The cells were cultured for 72 hours, harvested, and flow cytometry analysis performed to assess B-cell Ki-67 expression (A), FSC as a measure of relative cell size (B), cell-surface NOTCH2 expression (C), and number of live cells (D). (E-F) B cells from HCT patients with active cGVHD (n = 4) were plated in medium on monolayers of OP9-DL1 feeder cells and exposed to ATRA (0.1 μM), vehicle alone, anti-N2 mAb, or isotype control mAb. Following an initial culture period of 30 minutes, agonistic anti-IgM Ab was then added to the appropriate wells at a final concentration of 0.625 μg/mL. The cells were cultured for 72 hours, harvested, and flow cytometry analysis performed to assess B-cell surface proteins (E) and intracellular ERK1/2 protein phosphorylation (F). (E) Panel i shows representative dot plots from 1 patient for the treatments indicated; panel ii shows the frequency of $CD38^{+}IgD^{-}$ B cells from all 4 patients under the indicated culture conditions. (F) Panel i shows representative histograms from 1 patient for the treatments indicated; panel ii shows phospho-ERK MFI levels in B cells from all 4 patients under the indicated culture conditions. *P* values were determined using a paired Student *t* test. n.s., not significant.

Table 4. NOTCH-associated pathway gene expression as assessed in the RNA-Seq analysis of cGVHD B cells after NOTCH2 blockade

Gene	↑ or ↓	$\log_2$ fold change	*P*	Adjusted *P*	Rank (of 12 880)
HES4	↓	−2.97	2.8×10^{-17}	1.8×10^{-13}	2
HES1	↓	−1.10	3.8×10^{-4}	.062	80
LFNG	↑	0.660	.001	.105	133
HDAC2	↓	−0.541	.014	.321	543
MFNG	↓	−0.525	.016	.339	622
EP300	—	0.667	.061	.454	1 737
MAML2	—	0.552	.119	.510	2 997
NOTCH2	—	0.371	.165	.550	3 867
DTX2	—	0.300	.262	.622	5 430
HDAC1	—	−0.101	.595	.828	9 259
DTX1	—	0.030	.926	.976	12 209
DTX4	—	0.026	.933	.979	12 269

cGVHD B cells after NOTCH2 blockade from the experiment described in Table 2. *P* values and adjusted *P* values are indicated. The numerical rank for each gene of all 12 880 genes expressed above background is also indicated, based on the adjusted *P* value score.

—, Not significantly changed by NOTCH2 blockade.

TLR9.[50] TLR9 is upregulated in normal memory B cells that are primed for recall immune responses.[51] Because ATRA enhances responsiveness to CpG stimulation of normal human B cells,[49,52] and accelerates mature splenic B-cell expansion after vaccination in normal mice,[53] we examined how ATRA affects purified, otherwise unmanipulated, cGVHD patient B cells. We found that along with *IRF4*, *PAX5* and *TLR9* expression were both significantly increased by ATRA (Figure 5A). There was also a notable increase in *XBP1*, but *BLIMP1* expression was unchanged by ATRA, pointing away from a plasma cell differentiation program. These data reveal that cGVHD patient B cells have potential functional "plasticity" that may be alterable in vivo.

Having found that ATRA induced *TLR9* in cGVHD B cells, we investigated whether this effect was associated with an augmented response to CpG. As shown in Figure 5B, the frequency of B cells with a plasmablast-like phenotype (Ki-67$^+$CD19^{low}FSC^{high}) induced by CpG stimulation alone, or by CpG plus anti-IgM, was sixfold greater with the addition of ATRA. Notably, this ATRA-induced plasmablast-like phenotype was not accompanied by additional changes in overall cell size (Figure 5C). These findings indicate a potential to restore B-cell function because plasmablast-like cells from patients with cGVHD have known marked attenuation of CpG-induced signaling compared with cells from patients without cGVHD.[54]

ATRA attenuates BCR-NOTCH2 hyperresponsiveness in cGVHD B cells

IRF4 exerts a suppressive effect on NOTCH signaling in B cells.[42] Thus, we examined whether the enhancement of IRF4 by ATRA culminated in the suppression of cGVHD B-cell hyperresponsiveness to NOTCH2-BCR stimulation. ATRA treatment resulted in almost complete suppression of cGVHD B-cell activation by NOTCH2-BCR stimulation (Figure 6A), along with a reduction in B-cell size (Figure 6B). The modest activation induced by NOTCH ligand without the addition of anti-IgM was also significantly reduced by ATRA (Figure 6A). These data reveal that ATRA potently reverses the NOTCH2 hyperresponsiveness of cGVHD B cells established in vivo. Because NOTCH2 expression was maintained on the surface of active cGVHD B cells during NOTCH2-BCR engagement (Figure 2A), we investigated whether ATRA affected this process. Surface NOTCH2 indeed decreased with ATRA (Figure 6C), similar to the decrease seen when SYK inhibitor R406 blocks BCR signaling (Figure 6C). Importantly, ATRA treatment did not reduce overall B-cell viability in these assays (Figure 6D). Instead, ATRA suppressed the expansion of a "post-germinal center" CD38$^+$IgD$^-$ B-cell subset[14] (Figure 6Ei-ii). ATRA, as well as anti-N2, also reduced low-level IgM production after NOTCH2-BCR stimulation (supplemental Figure 4). ERK1/2 MAPK phosphorylation is necessary for BCR signaling, but is transient, subsiding within hours of BCR ligation.[55,56] ERK1/2 phosphorylation remained detectable in cGVHD B cells cultured without anti-IgM, but was reduced in the presence of anti-IgM (Figure 6Fi-ii). ATRA did not alter this reduction in ERK1/2 phosphorylation, suggesting it affects the BCR pathway further downstream. Thus, ATRA blocks NOTCH2 expression and B-cell hyperactivation, while affording functional responsiveness in pathways.

Discussion

cGVHD has become the most important long-term sequela facing cancer survivors of allogeneic HCT, and disease mechanisms are emerging.[57] Having demonstrated a role for BCR-activated cells in the pathophysiology of cGVHD,[6,7,12] we now show that NOTCH2 activation is pivotal for aberrant BCR activation in this disease. Our study begins to elucidate potentially targetable molecular underpinnings of B-cell pathology in cGVHD.

After HCT, B cells are constantly exposed to alloantigens. In cGVHD, potentially pathologic B-cells are promoted to survive through constitutive signaling via BCR and BAFF-associated pathways.[5-7] We now demonstrate that cGVHD B cells have remarkable sensitivity to limiting amounts of BCR ligand when NOTCH2 is also activated (Figures 1-3). Our data show that NOTCH2 is a potent costimulator of aberrant BCR responses in cGVHD. Importantly, alloantigen appears to prime cGVHD patient B cells in vivo to receive NOTCH signals. Even without ex vivo BCR stimulation, NOTCH activation was significantly increased in cGVHD B cells (Figure 1C). BLNK was also increased in cGVHD B cells following NOTCH-BCR

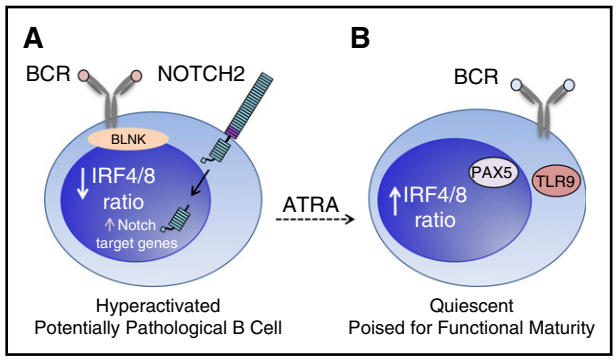

Figure 7. Model for a NOTCH2-BCR axis in the generation of pathogenic B cells in cGVHD. (A) Reduced activation threshold response to antigen and to NOTCH ligand. High BAFF levels in the cGVHD setting leads to the preferential survival of B cells with MZ-like properties. These B cells are driven by an abnormally low ratio of IRF4 to IRF8, and are dependent on NOTCH2 activation of target genes. BCR-NOTCH2 synergy in these B cells leads to pathogenic Allo-Ab production. (B) ATRA exposure normalizes the phenotype of cGVHD B cells by increasing the ratio of IRF4 to IRF8, eliminating NOTCH2 dependence. This in turn leads to enhanced expression of PAX5 and TLR9, a genetic profile associated with mature follicular B cells capable of producing protective Ab against bacteria and viruses, as well as to vaccines. Importantly, these B cells attain functional memory essential for long-term humoral immunity.

stimulation (Figure 1D-E), providing evidence that a NOTCH2-BCR axis operates from the most proximal steps of BCR signaling. NOTCH2 may play a role in how cGVHD B cells are primed to respond to alloantigens because anti-N2 blocked active cGVHD B-cell hyperresponsiveness (Figure 2A). In the face of this inappropriate activation signaling, cGVHD B cells appear unable to mature normally. Our findings may partially explain humoral immune dysregulation and profound immunodeficiency common in cGVHD.[58]

NOTCH2 blockade of active cGVHD B cells also led to the downregulation of genes associated with MZ B cells (Tables 2-3), including *CR2/CD21*[59] and *FCRL4/IRTA1*,[60] supporting our hypothesis that circulating B cells in cGVHD patients share characteristics with MZ-like B cells. The glycosyltransferase *MFNG* (*MANIC FRINGE*), important for MZ-like B-cell promotion by NOTCH2,[41] was significantly reduced following NOTCH2 blockade (Figure 2C; Table 4). NOTCH2 blockade was not coincident with complete abrogation of cell-activation pathways. *FOS* was among the genes upregulated in cGVHD B cells after NOTCH2 blockade (Tables 2-3), supporting the previously published role for FOS in suppressing BCR-mediated proliferation,[61] and this accompanied an overall enhancement of the MAPK-signaling pathway (supplemental Figure 1B; supplemental Table 3). FOS can participate in BLIMP1 expression and antibody-secreting cell (ASC) differentiation.[62] However, ASCs were not generated following NOTCH2 blockade of cGVHD B cells, and BLIMP1 expression was not significantly altered (RNA-Seq; $P = .2$). These findings are consistent with anti-N2 attenuating hyperactivation, poising cGVHD B cells for receipt of additional signals needed for ASC differentiation.[62]

Consistent with findings by others, NOTCH2 expression is only detectable at modest levels on the B-cell surface.[42] Low-level NOTCH2 expression and posttranslational modifications of its extracellular domain by FRINGE glycosyltransferases[41] are known to be sufficient for potent downstream NOTCH signaling and the development of autoreactive-prone MZ B cells.[41,42] We also reveal a positive feedback loop underpinning NOTCH2 expression and activation. BCR activation in cGVHD associated with low levels of the transcription factor IRF4 and increased NOTCH2 cell-surface expression. IRF4 is known to be required for MZ B-cell formation by NOTCH2.[28,29] Strikingly, with NOTCH-BCR stimulation, NOTCH2 expression was maintained on cGVHD B cells, and ATRA treatment blocked this effect (Figure 6C). This suggests that targeting NOTCH2 as B cells encounter alloantigen and NOTCH ligand may be possible.

We found that reduced IRF4 associated with a relative increase in IRF8 in active cGVHD B cells stimulated with surrogate antigen (Figure 4). This is an important finding because BCR signaling is a primary driver of changes in *IRF4* and *IRF8* expression during B-cell development and activation, and a strict balance between IRF4 and IRF8 controls the emergence of major B-cell subsets in the peripheral B-cell pool.[44,48,63] In conjunction with IRF4, IRF8 is also a crucial mediator of B-cell tolerance.[45,64] These findings suggest that intrinsic transcription factor defects occur in surviving and potentially autoreactive B cells after HCT (Figure 7A), and that ATRA may normalize B-cell function (Figure 7B).

The B-cell maturation defect we have uncovered in cGVHD patients may lend itself to therapeutic intervention. ATRA induced a maturation program in cGVHD B cells that included increased *IRF4*, *TLR9*, and *PAX5* expression and enhanced CpG responses (Figures 5 and 7B), consistent with findings by others in healthy and common variable immunodeficiency human B cells.[49,52] ATRA enhances B-cell maturation from lymphoid progenitors in vitro and expands splenic B cells in mice after vaccination.[52,65] Agents that enable entry into B-cell maturation pathways may eliminate autoreactive B cells, in favor of mature follicular B cells functional against pathogens. Retinoids have been used clinically in human disease, both for treating acute promyelocytic leukemia and for augmenting immunity.[66,67] In a limited case series, etretinate, a retinoid used in psoriasis, showed some efficacy in sclerodermatous cGVHD.[68] Likewise, the ATRA-like retinoid Am80 reduced cutaneous cGVHD in a mouse model,[69] potentially through modulation of effector T cells, although a possible role for B cells was also acknowledged, but not examined. Collectively, our findings now suggest that retinoids and similar agents that modulate immune cell function warrant further study in cGVHD.

Acknowledgments

The authors thank Jerome Ritz of the Dana-Farber Cancer Institute for some of the invaluable deidentified patient samples, Rigel Pharmaceuticals for providing R406, and Zhiguo Li for help with statistics.

This work was supported by grants from the Leukemia & Lymphoma Society (6497-16 [S.S.], 6462-15 [B.R.B. and I.M.]); by the US Department of Defense (W81XWH-11-1-0537 [S.S.]); and by the National Institutes of Health: R01 HL 129061-01 (National Heart, Lung, and Blood Institute [S.S.]), R01 AI 091627 (National Institute of Allergy and Infectious Diseases [I.M.]), and P01C142106 and R01AI34495 (National Cancer Institute and National Institute of Allergy and Infectious Diseases [B.R.B.]).

Authorship

Contribution: J.C.P., W.J., and S.S. designed the study and wrote the paper; I.M., C.W.S., and B.R.B. provided scientific advice and reviewed the paper; J.C.P., W.J., H.S., A.N.S., P.V.T., and B.G.V. performed the experiments; S.A., J.J.R., J.S.S., S.Z.P., F.T.H., M.E.H., V.T.H., and N.J.C. provided patient samples and edited the paper; C.D.J. and P.F.K. performed and analyzed BCR high-throughput sequencing; and K.O. and D.Z. performed preprocessing and differential expression analysis of the RNA-Seq and NanoString data.

Conflict-of-interest disclosure: The authors declare no competing financial interests.

ORCID profiles: J.C.P., 0000-0002-7789-1564; C.D.J., 0000-0001-7281-7130; P.F.K., 0000-0001-7861-916X; J.S.S., 0000-0003-4568-1092; M.E.H., 0000-0001-9863-8464; S.Z.P., 0000-0001-9111-9354; F.T.H., 0000-0003-2507-8229; D.Z., 0000-0002-4641-786X; K.O., 0000-0002-3340-1287; B.R.B., 0000-0002-9608-9841; N.J.C., 0000-0001-6725-7220; I.M., 0000-0003-1312-6748; S.S., 0000-0003-4551-6687.

Correspondence: Stefanie Sarantopoulos, Duke Adult Bone Marrow, 2400 Pratt St, Suite 9000, DUMC Box 3961, Durham, NC 27710; e-mail: stefanie.sarantopoulos@duke.edu.

References

1. Cutler CS, Koreth J, Ritz J. Mechanistic approaches for the prevention and treatment of chronic GVHD. *Blood*. 2017;129(1):22-29.
2. MacDonald KP, Hill GR, Blazar BR. Chronic graft-versus-host disease: biological insights from preclinical and clinical studies. *Blood*. 2017; 129(1):13-21.
3. Gea-Banacloche J, Komanduri KV, Carpenter P, et al. National Institutes of Health Hematopoietic Cell Transplantation Late Effects Initiative: The Immune Dysregulation and Pathobiology Working Group Report. *Biol Blood Marrow Transplant*. 2017;23(6):870-881.
4. Tivol E, Komorowski R, Drobyski WR. Emergent autoimmunity in graft-versus-host disease. *Blood*. 2005;105(12):4885-4891.
5. Allen JL, Fore MS, Wooten J, et al. B cells from patients with chronic GVHD are activated and primed for survival via BAFF-mediated pathways. *Blood*. 2012;120(12):2529-2536.
6. Allen JL, Tata PV, Fore MS, et al. Increased BCR responsiveness in B cells from patients with chronic GVHD. *Blood*. 2014;123(13):2108-2115.
7. Dubovsky JA, Flynn R, Du J, et al. Ibrutinib treatment ameliorates murine chronic graft-versus-host disease. *J Clin Invest*. 2014;124(11): 4867-4876.
8. Flynn R, Du J, Veenstra RG, et al. Increased T follicular helper cells and germinal center B cells are required for cGVHD and bronchiolitis obliterans. *Blood*. 2014;123(25):3988-3998.
9. Forcade E, Kim HT, Cutler C, et al. Circulating T follicular helper cells with increased function during chronic graft-versus-host disease. *Blood*. 2016;127(20):2489-2497.
10. Cooke KR, Luznik L, Sarantopoulos S, et al. The biology of chronic graft-versus-host disease: a task force report from the National Institutes of Health Consensus Development Project on Criteria for Clinical Trials in Chronic Graft-versus-Host Disease. *Biol Blood Marrow Transplant*. 2017;23(2):211-234.
11. Sarantopoulos S, Blazar BR, Cutler C, Ritz J. B cells in chronic graft-versus-host disease. *Biol Blood Marrow Transplant*. 2015;21(1):16-23.
12. Flynn R, Allen JL, Luznik L, et al. Targeting Syk-activated B cells in murine and human chronic graft-versus-host disease. *Blood*. 2015;125(26): 4085-4094.
13. Matsuoka K, Kim HT, McDonough S, et al. Altered regulatory T cell homeostasis in patients with CD4+ lymphopenia following allogeneic hematopoietic stem cell transplantation. *J Clin Invest*. 2010;120(5):1479-1493.
14. Sarantopoulos S, Stevenson KE, Kim HT, et al. Altered B-cell homeostasis and excess BAFF in human chronic graft-versus-host disease. *Blood*. 2009;113(16):3865-3874.
15. Sarantopoulos S, Ritz J. Aberrant B-cell homeostasis in chronic GVHD. *Blood*. 2015; 125(11):1703-1707.
16. Avanzini MA, Locatelli F, Dos Santos C, et al. B lymphocyte reconstitution after hematopoietic stem cell transplantation: functional immaturity and slow recovery of memory CD27+ B cells. *Exp Hematol*. 2005;33(4):480-486.
17. Miklos DB, Kim HT, Miller KH, et al. Antibody responses to H-Y minor histocompatibility antigens correlate with chronic graft-versus-host disease and disease remission. *Blood*. 2005; 105(7):2973-2978.
18. Miklos DB, Kim HT, Zorn E, et al. Antibody response to DBY minor histocompatibility antigen is induced after allogeneic stem cell transplantation and in healthy female donors. *Blood*. 2004;103(1):353-359.
19. Zorn E, Miklos DB, Floyd BH, et al. Minor histocompatibility antigen DBY elicits a coordinated B and T cell response after allogeneic stem cell transplantation. *J Exp Med*. 2004; 199(8):1133-1142.
20. Cordonnier C, Labopin M, Robin C, et al. Long-term persistence of the immune response to antipneumococcal vaccines after Allo-SCT: 10-year follow-up of the EBMT-IDWP01 trial. *Bone Marrow Transplant*. 2015;50(7):978-983.
21. Kalhs P, Panzer S, Kletter K, et al. Functional asplenia after bone marrow transplantation. A late complication related to extensive chronic graft-versus-host disease. *Ann Intern Med*. 1988; 109(6):461-464.
22. Ljungman P, Lewensohn-Fuchs I, Hammarström V, et al. Long-term immunity to measles, mumps, and rubella after allogeneic bone marrow transplantation. *Blood*. 1994;84(2):657-663.
23. Greinix HT, Pohlreich D, Kouba M, et al. Elevated numbers of immature/transitional CD21- B lymphocytes and deficiency of memory CD27+ B cells identify patients with active chronic graft-versus-host disease. *Biol Blood Marrow Transplant*. 2008;14(2):208-219.
24. Kuzmina Z, Krenn K, Petkov V, et al. CD19(+) CD21(low) B cells and patients at risk for NIH-defined chronic graft-versus-host disease with bronchiolitis obliterans syndrome. *Blood*. 2013; 121(10):1886-1895.
25. Gorelik L, Gilbride K, Dobles M, Kalled SL, Zandman D, Scott ML. Normal B cell homeostasis requires B cell activation factor production by radiation-resistant cells. *J Exp Med*. 2003;198(6): 937-945.
26. Magri G, Miyajima M, Bascones S, et al. Innate lymphoid cells integrate stromal and immunological signals to enhance antibody production by splenic marginal zone B cells. *Nat Immunol*. 2014;15(4):354-364.
27. Thien M, Phan TG, Gardam S, et al. Excess BAFF rescues self-reactive B cells from peripheral deletion and allows them to enter forbidden follicular and marginal zone niches. *Immunity*. 2004;20(6):785-798.
28. Descatoire M, Weller S, Irtan S, et al. Identification of a human splenic marginal zone B cell precursor with NOTCH2-dependent differentiation properties [*J Exp Med*. 2014;21(5): 1005]. *J Exp Med*. 2014;211(5):987-1000.
29. Saito T, Chiba S, Ichikawa M, et al. Notch2 is preferentially expressed in mature B cells and indispensable for marginal zone B lineage development. *Immunity*. 2003;18(5):675-685.
30. Carey JB, Moffatt-Blue CS, Watson LC, Gavin AL, Feeney AJ. Repertoire-based selection into the marginal zone compartment during B cell development. *J Exp Med*. 2008;205(9): 2043-2052.
31. Wen L, Brill-Dashoff J, Shinton SA, Asano M, Hardy RR, Hayakawa K. Evidence of marginal-zone B cell-positive selection in spleen. *Immunity*. 2005;23(3):297-308.
32. Thomas M, Calamito M, Srivastava B, Maillard I, Pear WS, Allman D. Notch activity synergizes with B-cell-receptor and CD40 signaling to enhance B-cell activation. *Blood*. 2007;109(8):3342-3350.
33. Chung J, Ebens CL, Perkey E, et al. Fibroblastic niches prime T cell alloimmunity through Delta-like Notch ligands. *J Clin Invest*. 2017;127(4): 1574-1588.
34. Lin KI, Angelin-Duclos C, Kuo TC, Calame K. Blimp-1-dependent repression of Pax-5 is required for differentiation of B cells to immunoglobulin M-secreting plasma cells. *Mol Cell Biol*. 2002;22(13):4771-4780.
35. Rookhuizen DC, DeFranco AL. Toll-like receptor 9 signaling acts on multiple elements of the germinal center to enhance antibody responses. *Proc Natl Acad Sci USA*. 2014;111(31): E3224-E3233.
36. Shaffer AL, Lin KI, Kuo TC, et al. Blimp-1 orchestrates plasma cell differentiation by extinguishing the mature B cell gene expression program. *Immunity*. 2002;17(1):51-62.
37. Wu Y, Cain-Hom C, Choy L, et al. Therapeutic antibody targeting of individual Notch receptors. *Nature*. 2010;464(7291):1052-1057.
38. Boyd SD, Marshall EL, Merker JD, et al. Measurement and clinical monitoring of human lymphocyte clonality by massively parallel VDJ pyrosequencing. *Sci Transl Med*. 2009;1(12): 12ra23.
39. Fabbri G, Holmes AB, Viganotti M, et al. Common nonmutational NOTCH1 activation in chronic lymphocytic leukemia. *Proc Natl Acad Sci USA*. 2017;114(14):E2911-E2919.
40. Benjamini Y, Hochberg Y. Controlling the false discovery rate - a practical and powerful approach to multiple testing. *J R Stat Soc B*. 1995;57(1): 289-300.
41. Tan JB, Xu K, Cretegny K, et al. Lunatic and manic fringe cooperatively enhance marginal zone B cell precursor competition for delta-like 1 in splenic endothelial niches. *Immunity*. 2009; 30(2):254-263.
42. Simonetti G, Carette A, Silva K, et al. IRF4 controls the positioning of mature B cells in the lymphoid microenvironments by regulating NOTCH2 expression and activity. *J Exp Med*. 2013;210(13):2887-2902.
43. Ochiai K, Maienschein-Cline M, Simonetti G, et al. Transcriptional regulation of germinal center B and plasma cell fates by dynamical control of IRF4. *Immunity*. 2013;38(5):918-929.
44. Xu H, Chaudhri VK, Wu Z, et al. Regulation of bifurcating B cell trajectories by mutual antagonism between transcription factors IRF4 and IRF8. *Nat Immunol*. 2015;16(12):1274-1281.
45. Pathak S, Ma S, Shukla V, Lu R. A role for IRF8 in B cell anergy. *J Immunol*. 2013;191(12): 6222-6230.
46. Klein U, Casola S, Cattoretti G, et al. Transcription factor IRF4 controls plasma cell differentiation and class-switch recombination. *Nat Immunol*. 2006; 7(7):773-782.
47. Ma S, Turetsky A, Trinh L, Lu R. IFN regulatory factor 4 and 8 promote Ig light chain kappa locus activation in pre-B cell development. *J Immunol*. 2006;177(11):7898-7904.
48. Sciammas R, Shaffer AL, Schatz JH, Zhao H, Staudt LM, Singh H. Graded expression of interferon regulatory factor-4 coordinates isotype switching with plasma cell differentiation. *Immunity*. 2006;25(2):225-236.
49. Indrevær RL, Moskaug JO, Paur I, et al. IRF4 is a critical gene in retinoic acid-mediated plasma cell formation and is deregulated in common variable immunodeficiency-derived B cells. *J Immunol*. 2015;195(6):2601-2611.
50. Turner M, Mee PJ, Costello PS, et al. Perinatal lethality and blocked B-cell development in mice lacking the tyrosine kinase Syk. *Nature*. 1995; 378(6554):298-302.
51. Bernasconi NL, Onai N, Lanzavecchia A. A role for Toll-like receptors in acquired immunity: up-regulation of TLR9 by BCR triggering in naive B cells and constitutive expression in memory B cells. *Blood*. 2003;101(11):4500-4504.
52. Indrevær RL, Holm KL, Aukrust P, et al. Retinoic acid improves defective TLR9/RP105-induced immune responses in common variable

immunodeficiency-derived B cells. *J Immunol*. 2013;191(7):3624-3633.

53. Tangye SG, Bryant VL, Cuss AK, Good KL. BAFF, APRIL and human B cell disorders. *Semin Immunol*. 2006;18(5):305-317.
54. de Masson A, Bouaziz JD, Le Buanec H, et al. CD24(hi)CD27+ and plasmablast-like regulatory B cells in human chronic graft-versus-host disease. *Blood*. 2015;125(11):1830-1839.
55. Adem J, Hämäläinen A, Ropponen A, et al. ERK1/2 has an essential role in B cell receptor- and CD40-induced signaling in an in vitro model of germinal center B cell selection. *Mol Immunol*. 2015;67(2 Pt B):240-247.
56. Novak R, Jacob E, Haimovich J, Avni O, Melamed D. The MAPK/ERK and PI3K pathways additively coordinate the transcription of recombination-activating genes in B lineage cells. *J Immunol*. 2010;185(6):3239-3247.
57. Lee SJ, Klein JP, Barrett AJ, et al. Severity of chronic graft-versus-host disease: association with treatment-related mortality and relapse. *Blood*. 2002;100(2):406-414.
58. Boeckh M, Bowden RA, Storer B, et al. Randomized, placebo-controlled, double-blind study of a cytomegalovirus-specific monoclonal antibody (MSL-109) for prevention of cytomegalovirus infection after allogeneic hematopoietic stem cell transplantation. *Biol Blood Marrow Transplant*. 2001;7(6):343-351.
59. Timens W, Boes A, Poppema S. Human marginal zone B cells are not an activated B cell subset: strong expression of CD21 as a putative mediator for rapid B cell activation. *Eur J Immunol*. 1989; 19(11):2163-2166.
60. Miller I, Hatzivassiliou G, Cattoretti G, Mendelsohn C, Dalla-Favera R. IRTAs: a new family of immunoglobulinlike receptors differentially expressed in B cells. *Blood*. 2002; 99(8):2662-2669.
61. Kobayashi K, Phuchareon J, Inada K, et al. Overexpression of c-fos inhibits down-regulation of a cyclin-dependent kinase-2 inhibitor p27Kip1 in splenic B cells activated by surface Ig cross-linking. *J Immunol*. 1997;158(5):2050-2056.
62. Ohkubo Y, Arima M, Arguni E, et al. A role for c-fos/activator protein 1 in B lymphocyte terminal differentiation. *J Immunol*. 2005;174(12): 7703-7710.
63. Matsuyama T, Grossman A, Mittrücker HW, et al. Molecular cloning of LSIRF, a lymphoid-specific member of the interferon regulatory factor family that binds the interferon-stimulated response element (ISRE). *Nucleic Acids Res*. 1995;23(12): 2127-2136.
64. Pathak S, Ma S, Trinh L, Lu R. A role for interferon regulatory factor 4 in receptor editing. *Mol Cell Biol*. 2008;28(8):2815-2824.
65. Chen X, Esplin BL, Garrett KP, Welner RS, Webb CF, Kincade PW. Retinoids accelerate B lineage lymphoid differentiation. *J Immunol*. 2008;180(1): 138-145.
66. Matikainen S, Ronni T, Hurme M, Pine R, Julkunen I. Retinoic acid activates interferon regulatory factor-1 gene expression in myeloid cells. *Blood*. 1996;88(1):114-123.
67. Ross AC. Vitamin A supplementation and retinoic acid treatment in the regulation of antibody responses in vivo. *Vitam Horm*. 2007;75:197-222.
68. Marcellus DC, Altomonte VL, Farmer ER, et al. Etretinate therapy for refractory sclerodermatous chronic graft-versus-host disease. *Blood*. 1999; 93(1):66-70.
69. Nishimori H, Maeda Y, Teshima T, et al. Synthetic retinoid Am80 ameliorates chronic graft-versus-host disease by down-regulating Th1 and Th17. *Blood*. 2012;119(1):285-295.